An investigation of factors influencing freeze lining behaviour

Article *in* Mineral Processing and Extractive Metallurgy IMM Transactions section C · September 2017

DOI: 10.1080/03719553.2017.1375767

3 authors, including:

Tijl Crivits
Umicore
25 PUBLICATIONS **112** CITATIONS
SEE PROFILE

Peter Charles Hayes
eResearch Australasia - University of Queensland
411 PUBLICATIONS **10,218** CITATIONS
SEE PROFILE

This is an Accepted Manuscript of an article published by Taylor & Francis in Mineral Processing and Extractive Metallurgy: Transactions of the Institutions of Mining and Metallurgy on 31/08/2017, available online:
https://www.tandfonline.com/doi/abs/10.1080/03719553.2017.1375767

An Investigation of Factors influencing Freeze Lining Behaviour

Tijl Crivits[1], Peter C. Hayes[2], Evgueni Jak[2]

[1] *School of Chemical Engineering, University of Queensland, Brisbane, Australia (Currently Umicore Research, Olen, Belgium)*
[2]*School of Chemical Engineering, University of Queensland, Brisbane, Australia*

Corresponding author: Tijl Crivits
Address:
Umicore, Watertorenstraat 33
2250 Olen
Belgium
Email: tijlcrivits@gmail.com
Mobile phone: +32 473 765 719

Peter C. Hayes
Address:
School of Chemical Engineering
Level 4, Chemical Engineering Building (74)
The University of Queensland
Queensland 4072
Australia
Email: p.hayes@uq.edu.au
Mobile phone:

Evgueni Jak
Address:
School of Chemical Engineering
Level 4, Chemical Engineering Building (74)
The University of Queensland

Queensland 4072
Australia
Email: e.jak@uq.edu.au
Mobile phone:

An Investigation of Factors influencing Freeze Lining Behaviour

Recent studies have indicated that the steady state thicknesses and interface temperatures of freeze linings can be influenced by factors other than the thermal parameters of the systems. To explore these possibilities further cold modelling of freeze linings was undertaken in the CaCl2-H2O system using an experimental apparatus that enabled the variation of both the bath temperature and the fluid flow rate. Through in-situ experimental observations, it was shown that the phases formed, the deposit/liquid interface temperature and the freeze lining thicknesses depend strongly on chemical parameters and elementary reaction steps, which are not considered by the conventional thermal treatment of freeze linings. These results indicate the need for further systematic investigation of various process parameters that influence the elementary reaction steps that may be active in these systems under dynamic steady state conditions.

Keywords: freeze lining; $CaCl_2$-H_2O; cold modelling

Subject classification codes: include these here if the journal requires them

Introduction

Freeze linings

The conventional approach to the containment of aggressive molten slags in pyrometallurgical processes is to use high-density, high-melting temperature refractory materials that are in direct contact with the liquid. Under these hot-face conditions, in which containment material is at the same temperature as the bulk bath, the refractories progressively degrade and must be periodically replaced. The usable refractory life time is dependent on the rates of interactions between refractory and slag, which include the mechanisms of direct dissolution of refractory grains into the liquid slag or their removal through selective dissolution of the binding phase.

An alternative approach is the use of freeze linings in which a layer of solid bath material is deliberately formed on the surfaces and inner walls of high temperature

reactors to provide protection from these corrosive liquid slags. The technology involves extracting heat through the lining through cooling of one face of the lining. The freeze lining approach has been applied to the design of lances and to fixed walls in particularly aggressive environments to enable the processes to be successfully undertaken at an industrial scale (Marx, Shapiro & Henning, 2010, Fallah-Mehrjardi, Jansson, Taskinen, Hayes & Jak, 2014, Fallah-Mehrjardi, Hayes & Jak, 2014, Blancher, Sayasenh & Crespo, 2015). In these systems, the heat is transferred from the bulk slag to the deposit liquid interface, then through the thickness of the freeze lining and the outer wall of the reactor. The rate of heat transfer, Q_{FL}, from the bulk bath to the deposit liquid interface can be described by an equation of the form

$$Q_{FL} = h_{bath} A_{bath,FL} (T_{bath} - T_{bath,FL}) \quad (1)$$

where $T_{bath,FL}$ is the bath-freeze lining interface temperature, T_{bath} the bulk bath temperature, and h_{bath} the convective heat transfer coefficient of the bath (Fallah-Mehrjardi, Hayes & Jak, 2014). As such, the heat loss through the freeze lining (Q) is determined by the difference between the bulk bath temperature and the bath-freeze lining interface temperature, the interface area ($A_{bath,FL}$) and the convective heat transfer coefficient of the bath.

The heat loss through a planar furnace wall at steady state can also be described by an equation of the form

$$Q_{FL} = \frac{(T_{bath,FL} - T_{coolant})}{\frac{\Delta x_{FL,ss}}{A_{bath,FL} k_{FL}} + \frac{\Delta x_{cooling}}{A_{bath,FL} k_{cooling}} + \frac{1}{A_{bath,FL} h_{coolant}} + A_{bath,FL} R_{contact}} \quad (2)$$

where k_{FL} represents the thermal conductivity of the freeze lining, $T_{bath,FL}$ the bath-freeze lining interface temperature, $T_{coolant}$ the temperature of the coolant, T_{bath} the bulk bath temperature, $\Delta x_{cooling}$ the thickness of the cooling blocks, $k_{cooling}$ the thermal conductivity of the cooling blocks, $h_{coolant}$ the convective heat transfer coefficient between the coolant

and the cooling blocks and $R_{contact}$ the contact resistance between the cooling blocks and the freeze lining.

It is difficult to accurately predict from first principles the temperature profiles in these systems since the interface temperature and the thermal parameters are not strictly independent variables (Fallah-Mehrjardi, Hayes & Jak, 2013, Fallah-Mehrjardi, Hayes & Jak, 2013, Fallah-Mehrjardi, Hayes & Jak, 2013, Fallah-Mehrjardi, Hayes & Jak, 2014). As a first approximation, a number of simplifying assumptions can be made. For example, if under thermal steady state conditions the parameters are constant, and no refractory lining as in (Kalliala, Kaskiala, Suortti & Taskinen, 2015) is present, the steady state thickness of the freeze lining ($\Delta x_{FL,ss}$) can be described by equation **(3)** (Thonstad & Rolseth, 1983, Verscheure, Kyllo, Filzwieser, Blanpain & Wollants, 2006, Jansson, Taskinen & Kaskiala, 2014).

$$\Delta x_{FL,ss} = k_{FL}\left(\frac{(T_{bath,FL}-T_{coolant})}{h_{bath}(T_{bath}-T_{bath,FL})} - \left(\frac{\Delta x_{cooling}}{k_{cooling}} + \frac{1}{h_{coolant}} + R_{contact}\right)\right) \qquad (3)$$

Equations **(1)** and **(3)** show that both the steady state thickness of the lining and the heat loss through the lining are dependent on $T_{bath,FL}$. A number of approaches have been used to predict the growth and steady state thickness of freeze linings (Fallah-Mehrjardi, Hayes & Jak, 2014, Verscheure, Kyllo, Filzwieser, Blanpain & Wollants, 2006, Taylor & Welch, 1987, Pistorius, 2004, Zietsman, 2004, Guevara & Irons, 2011). In most of the previous predictions for thermal steady state conditions, the assumption has been made that the temperature at the bath-freeze lining interface equals the liquidus temperature of the bulk slag, and that the primary phase forms a dense sealing layer at this deposit/liquid interface. As a result of recent research on these systems, there is now extensive experimental evidence (Fallah-Mehrjardi, Jansson, Taskinen, Hayes & Jak, 2014, Fallah-Mehrjardi, Hayes & Jak, 2013, Fallah-Mehrjardi, Hayes & Jak, 2013,

Fallah-Mehrjardi, Hayes & Jak, 2013, Fallah-Mehrjardi, 2013, Fallah-Mehrjardi, Hayes & Jak, 2014) to demonstrate that the interface temperature can be below the liquidus and that the primary phase is not necessarily present at the deposit/liquid interface at thermal steady state conditions. These observations clearly indicate that to explain freeze lining behaviour, other factors, in addition to thermal parameters of the system, need to be considered.

Based on examination of freeze lining deposit/liquid interfaces and samples taken from slag baths prepared under a range of conditions, a general conceptual framework has been proposed (Fallah-Mehrjardi, Hayes & Jak, 2013) that can be used to explain the observed phenomena in a number of systems. The framework envisages dynamic steady state conditions in which crystallisation on detached crystals continuously takes place in the liquid as it moves towards the freeze lining deposit through a boundary layer below the liquidus temperature. The detached crystals approach local equilibrium with the liquid and, rather than becoming attached to the deposit, are returned to the bulk liquid through the action of turbulent eddies formed at the cooled deposit/liquid interface. These detached crystals are subsequently fully or partially dissolved upon moving back towards the bulk bath, which is maintained above the liquidus temperature.

Using this conceptual framework, it becomes clear that steady state freeze lining behaviour is determined by not only heat transfer and thermal factors, but also by the relative rates of mass transfer and elementary reaction steps, such as nucleation, crystallisation rate, crystallisation pathway, phase transformations and phase equilibria in the reaction system. The rate limiting step can be determined from the concentration and temperature profiles near the reaction interface. This is demonstrated in Figure 1 (Hayes, 2013).

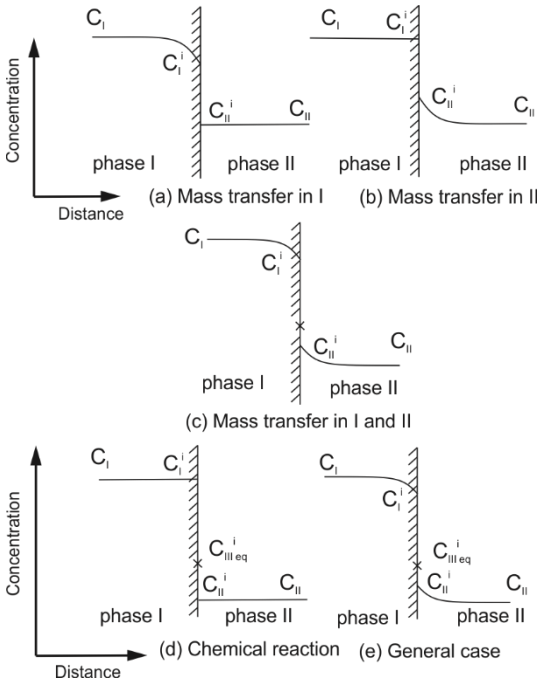

Figure 1: Schematic illustration of the solute concentration profiles across the interface between phases I and II; (a) mass transfer in phase I rate limiting; (b) mass transfer in phase II rate limiting; (c) mass transfer in phases I and II, both rate limiting; (d) chemical reaction at the interface between phases I and II rate limiting; and (e) general case. $C_{II}{}^{i}{}_{eq}$ is the concentration at the interface in phase II that would be in equilibrium with phase I at concentration C_I. Replicated from (Hayes, 2013)

A summary of factors influencing freeze lining behaviour can be found in Table 1. How they might influence the behaviour within different systems is briefly discussed in the following sections.

Heat transfer/thermal factors

The principal mechanisms of heat transfer are well established involving thermal diffusivity, natural convection and forced convection. These mechanisms all contribute to the overall heat transfer coefficient, h_{bath}, which is commonly described through the use of the dimensionless Nusselt number (Nu = f(Re,Pr,Gr)), where Re, Pr and Gr represent the Reynolds number, Prandtl number and Grashof number respectively. The

relationships between physical properties of the fluids and heat transfer for simple geometries have been established (Welty, Wicks, Wilson & Rorrer, 2007). Alternatively, computational fluid dynamic models are available to assist in estimating these values.

Whilst conduction and convection are the principal mechanisms of heat transfer in opaque systems, heat transfer can also take place through electromagnetic radiation through translucent materials (Gardon, 1961).

From equation **(1)**, it can be seen that the heat flux to the lining from the bulk bath is directly proportional to the temperature difference (T_{bath}-$T_{bath,FL}$) between the bath and the liquid bath/freeze lining interface. Through equation **(3)**, it can be determined that an increasing bath temperature will result in a reduction of the steady state freeze lining thickness.

All chemical reactions and phase transformations have enthalpy changes associated with them, either exothermic or endothermic. Locally, heat transfer mechanisms will take place in parallel with any chemical change.

Mass transfer/physical factors

Mass transfer takes place through analogous mechanisms to those described for heat transfer, involving contributions from mass diffusivity, natural convection and forced convection. The mass transfer coefficients are related to physical characteristics of the system through the Sherwood number (Sh = f(Re,Sc,Gr)) whith Re, Sc and Gr representing the Reynolds number, Schmidt number and Grashof number respectively (Welty, Wicks, Wilson & Rorrer, 2007).

Flow mechanisms, such as laminar and turbulent flow are also influenced by the relative

movements of solid and fluid phases, as well as local geometry.

In the context of the influence on freeze lining formation, these mass transfer mechanisms have the potential to influence, e.g. the rate of transfer of the fluid and detached crystals to and from the bulk liquid and the deposit liquid interface, the time of passage through the subliquidus region, and local mass transfer of solute to and from these detached crystals.

Elementary reaction steps/chemical factors

Having established that the deposit liquid interface can be less than the equilibrium liquidus temperature for the system, the relative rates of a number of different reaction steps must be considered. Some of these arise directly from consideration of the conceptual framework established in earlier research (Fallah-Mehrjardi, Hayes & Jak, 2013).

It is envisaged that primary phase crystals can form in the subliquidus layer ahead of the steady state interface. These crystals can form through homogeneous or heterogeneous nucleation mechanisms. The rate of nucleation depends on a number of factors, including the thermodynamic driving force (also expressed as local undercooling of the melt), solids composition and interfacial energy. In the case of heterogeneous nucleation, additional factors, such as pre-existing solids, % solids, and the composition and crystal structure of these solids can be important.

The rates of growth and dissolution of these crystals as they pass through the subliquidus layer should also be considered. The rate of crystal growth will be influenced by local undercooling and concentrations of the components in the solid and liquid phases.

As the crystals approach the deposit interface, the local temperature will decrease and the relative stabilities of solid phases that could be formed in the system will change. The crystallization path and the sequence of changes at the crystal surface depend on the shape of the liquidus, the shape of the solidus, maximum% of solids above the solidus, the extent of solid solutions and the change in composition of the liquid and solid phases with temperature.

There are different reasons why there may be no crystals that are formed ahead of the deposit interface, associated with slow nucleation and/or growth rates. In extreme conditions, the deposit interface may even be at or below the glass transition temperature T_g, in which case the deposit interface would consist of an amorphous or glassy phase (Campforts, Blanpain & Wollants, 2009).

In the deposit itself, phase transformations and secondary reactions may take place; in these cases the reaction will depend on the phases present, the phase compositions and the proportion of phases. The microstructures and associations of these new phases can influence physico-chemical properties of the deposit, such as the local thermal conductivity. The shapes of the phases, e.g. faceted/non-faceted crystals, can also have an effect on the microstructures formed and the resulting physico-chemical properties.

At subsolidus temperatures, some materials undergo polymorphic transformation or other transitions that can influence chemical or physical properties, e.g. release of gases from solution and changes in molar volume.

The rate-determining reaction step can often be distinguished based on the temperature and compositional profiles at the reaction interface (Figure 1). It will be clear from the many elementary reaction steps that can take place in these systems that many of the factors listed (Table 1) influence more than one process or reaction step.

Table 1: Potential elementary reaction steps and factors that influence steady state freeze lining behaviour.

	Heat transfer/ thermal factors	**Elementary reaction steps/ chemical factors**	**Mass transfer/ physical factors**
Bath	*Bulk heat transfer* Nu = f(Re,Pr,Gr) $(T_{bath}-T_{bath,FL})$ - Natural convection - Forced convection - h_{bath} - $c_{p,bath}$ - k_{bath} • k_{phonon} • $k_{radiation}$ • $k_{electronic}$ - ρ_{bath} - Geometry	*Homogeneous nucleation rate* - Solids composition - Undercooling - Interfacial energy *Heterogeneous nucleation rate* - Pre-existing solids - % solids - Crystal structure *Crystallization rate* - Undercooling - Mass diffusivity - Natural convection - Forced convection *Crystallization path* - Shape of liquidus - Shape of solidus - Max% of solids above solidus - Solid solutions *Glass transition temperature, T_g*	*Bulk flow* - Sh = f(Re,Sc,Gr) - Mass diffusivity - Natural convection - Forced convection *Local flow* - Geometry
Freeze lining	k_{FL} - porosity - phases present - phase	*Phase transformations/reactions* - phases present - phase compositions	

	proportions - microstructure	- phase proportions - microstructure, faceted/non-faceted crystals - phase transition temperature - change in molar volume - chemical reactions	
Cooling blocks	$k_{cooling}$ Geometry		
Coolant	$T_{coolant}$ $h_{coolant}$ - $c_{p,coolant}$ - $k_{coolant}$ - $\rho_{coolant}$		

Only some of these factors have been investigated to date

Heat transfer

The effect of heat transfer on the steady state freeze lining behaviour is well established by previous research (Thonstad & Rolseth, 1983, Verscheure, Kyllo, Filzwieser, Blanpain & Wollants, 2006, Taylor & Welch, 1987, Solheim & Thonstad, 1983, Solheim & Thonstad, 1984, Bruggeman & Danka, 1990, Chen, Wei, Thomson, Welch & Taylor, 1994, Valles & Lenis, 1995, Wei, Chen, Welch & Voller, 1997, Solnordal, Jorgensen & Taylor, 1998, Robertson & Kang, 1999, Thonstad, Fellner, Haarberg, Hives, Kvande & Sterten, 2001, Solheim, 2003, Solheim, 2011), and has been summarized in the introduction.

Mass transfer

The effect of bath agitation on freeze lining behaviour has been investigated (Fallah-

Mehrjardi, Hayes & Jak, 2013). Increasing bath agitation was found to increase the liquid bath/deposit interface temperature and result in a denser interface structure, containing a higher proportion of solids. The steady state thickness decreased and the steady state heat flux increased with increasing bath agitation.

(Guevara & Irons, 2011) demonstrated the effect of the bulk fluid flow. The freeze lining is thinnest at the position at which the fluid arrives from the bulk bath at the freeze lining interface. The longer the fluid travels across the freeze lining interface, the thicker the freeze lining becomes. This change in thickness can be attributed to two causes. Firstly, the temperature of the liquid is higher at the top than at the bottom due to thermal stratification. Secondly, the natural convective boundary layer grows thicker the longer the liquid travels along the freeze lining.

Liquidus temperature

(Thonstad & Rolseth, 1983) studied the effect of changes in liquidus temperature, using a solution of stearic acid and myristic acid, as well as plant observations in aluminium processing. It was found that, as the liquidus temperature of the bath is changed, the bath temperatures shifts in the same direction. This was attributed to the achievement of thermal balance. As long as the heat input stays constant in a closed system, the heat loss - through the freeze lining - has to stay constant as well in. Equation **(1)** demonstrates that this requires the superheat ($T_{bath} - T_{bath,FL}$) to stay constant. As the bath-freeze lining interface equalled the liquidus temperature in the investigated systems, the bath temperature has to shift in the same direction as the liquidus temperature to achieve a constant superheat.

Chemical composition

(Campforts, Blanpain & Wollants, 2009) investigated the microstructure of six synthetic lead slags to demonstrate the importance of slag engineering in the optimization of freeze lining behaviour. While most slag systems formed freeze linings consisting of several (partially) crystalline layers, the slag system containing the highest concentration of silica was found to form a glassy freeze lining, containing only a few microcrystals.

(Fallah-Mehrjardi, Jansson, Taskinen, Hayes & Jak, 2014, Fallah-Mehrjardi, Hayes & Jak, 2014, Fallah-Mehrjardi, Hayes & Jak, 2013, Fallah-Mehrjardi, Hayes & Jak, 2013, Fallah-Mehrjardi, Hayes & Jak, 2013, Fallah-Mehrjardi, 2013, Fallah-Mehrjardi, Hayes & Jak, 2014) studied freeze linings in the Al_2O_3-'Cu_2O'-'Fe_2O_3'-SiO_2, calcium ferrite, cryolite and industrial lead slag systems. Depending on the system, the interface temperature ranged from the solidus temperature to the liquidus temperature. In one particular study , it was shown that slightly decreasing the silica content of a slag by approximately 6 wt.% could cause a transition of the interface temperature from below the liquidus to the liquidus temperature.

Superheat, undercooling

(Guevara & Irons, 2011) studied the effect of changing superheat on freeze lining behaviour in the $CaCl_2$-H_2O system. The steady state thickness of the freeze lining was found to decrease with increasing superheat. The liquid bath/deposit interface was found to be equal to the solidus temperature in all experiments.

(Fallah-Mehrjardi, Hayes, Vervynckt & Jak, 2014) observed the presence of solids in the bulk bath liquid during freeze lining experiments in a non-ferrous industrial slag.

Based on this, it was suggested that freeze linings could possibly be created while operating at subliquidus bath temperatures.

Methodology

Experimental apparatus

Undertaking experimental studies at high temperature using metallurgical slag systems is difficult and time consuming, and it is not possible to observe the phenomena taking place at the deposit/liquid interface. In the present study, the approach used earlier (Guevara & Irons, 2011) of using a cold model to investigate the effects of different factors on freeze lining formation has been adopted. The detailed design of the apparatus used in the present study differs slightly from that used in earlier research (Guevara & Irons, 2011). Figure 2 shows the experimental apparatus in which aqueous solution containing $CaCl_2$ flows over a water-cooled copper plate. The freeze lining deposit forms on the surface of the plate and the process is continuously observed through the transparent wall of the reactor. The reactor consists of a tank made from acrylic sheet (inside dimensions 30 cm length, 5 cm width, 10 cm height, 1 cm wall thickness) surrounded on three sides, the top and the bottom by 3 cm thick polystyrene foam insulation. The fourth side, along the length of the bath, was made of a double layer of acrylic sheet with a 1 cm air gap in between. A removable lid containing a 2 mm wide slit across the length of the lid allowed temperature measurements to be made using thermocouples without removal of the lid. A copper cooling plate with cooling circuit welded on the back, through which tap water at room temperature was run, was used on the cold side of the tank. To direct the solution flow to the surface of the copper plate, a 2 mm thick acrylic plate was positioned horizontally in the middle of the tank, leaving a 5 cm gap between the cooled copper circuit and the acrylic plate. The forced

circulation of the aqueous solution along the tank above the acrylic dividing plate was achieved using an electrically driven peristaltic pump (Masterflex console drive + Masterflex Easyload head, model 7518-10, ColePalmer, USA) with Masterflex Norprene tubing (A60 G, L/S 18). The solution exited the tank at the opposite end to the water-cooled plate. The bulk solution was heated in a separate copper tank (10x10x10 cm, 1mm wall thickness) containing a spiral shaped titanium heating element (240V, 200 W, 40 mm OD, 75 mm height).

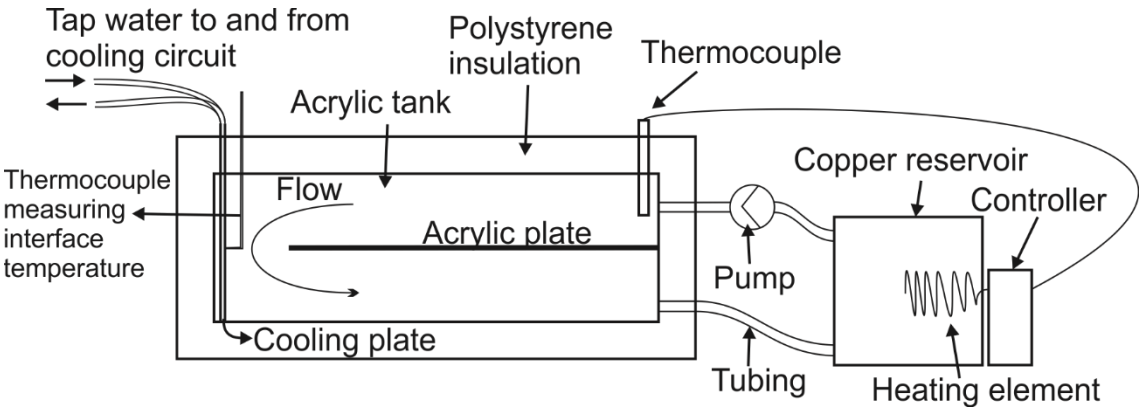

Figure 2: Schematic of the experimental apparatus.

A 0 – 120 °C bulb/capillary type thermostat was used to control the bath temperature within ±0.5 °C. The temperatures in the bath were measured using thin K-type thermocouples (⌀ 1 mm, ECEFAST, Australia). A similar thermocouple was used to measure the interface temperature. To provide more accurate interface temperature measurements, the stainless steel protective sheath was stripped back from this thermocouple, exposing the thermocouple tip. All thermocouples were calibrated against the controller thermocouple before each measurement. The temperature of the tap water was found to be approximately 20 °C and varied within ±1 °C over the course of each experiment.

Experimental procedure

Distilled water and $CaCl_2.2H_2O$ (>99% purity, Sigma Aldrich) were mixed in the

acrylic tank. The tank was closed and heated to 50 °C while applying a solution flow rate of 875 ml/min. The acrylic tank was left over night until all the $CaCl_2.2H_2O$ had dissolved. The bath was cooled until the desired bath temperature was reached and the solution flow rate was adjusted to the desired experimental value, after which the cooling water to the copper plate was turned on. Images of the thickness of the freeze lining deposit were recorded through the transparent side of the acrylic tank using a digital camera, positioned approximately 0.5 m from the acrylic tank. The thickness of the freeze lining was measured using the ImageJ software (Rasbane, 1997-2015). The same grid cell was chosen as scale on each image. The distance from the freeze lining interface to a set vertical grid line was measured. Subtracting this value from the distance of this vertical grid line to the cooling plate measured in the initial image yielded the freeze lining thickness.

Temperatures at the interface were measured at specific positions (Figure 10) at specific times, with larger intervals between measurements as the experiment progressed and the freeze lining grew more slowly. The temperature was measured by pressing the stripped K-type thermocouple against the interface for approximately 30 seconds. This was the observed time necessary for the thermocouple to reach thermal steady state with its surroundings in those conditions where the freeze lining growth in this time frame was negligible.

The $CaCl_2$-H_2O system

Figure 3 shows the phase diagram of the CaCl2-H2O system from -60 to +80 °C and 0 to 80 wt. % CaCl2 (Conde-Petit, 2014). In this composition range, four solid compounds are present: congruently melting ice (H2O), and incongruently melting CaCl2.6H2O (50.7 wt.% CaCl2), CaCl2.4H2O (60.6 wt.% CaCl2) and CaCl2.2H2O

(75.5 wt.% CaCl2).

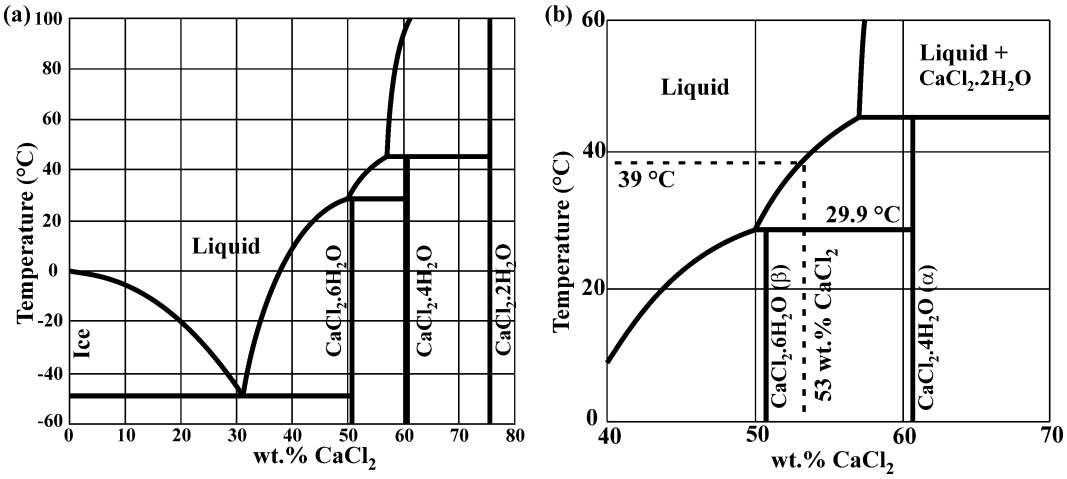

Figure 3: (a) Phase diagram of the $CaCl_2$-H_2O system; (b) Close-up of the conditions of interest for the current study.

For experimental convenience, initially a 53 wt.% $CaCl_2$ solution was selected for the study, equal to the solution selected in previous research (Guevara & Irons, 2011). Upon equilibrium cooling of this solution, the $CaCl_2.4H_2O$ solid primary phase (α) precipitates out of the liquid at approximately 39 °C. Upon reaching the solidus temperature of 29.9 °C (DOWChemical, 2002), a peritectic reaction between the liquid and the primary phase results in the formation of solid $CaCl_2.6H_2O$; this secondary phase will be referred to as (β) in the following figures.

To examine the effect of solution composition, the behaviour of a 52 wt.% $CaCl_2$ solution was also examined. The crystallization path of this solution is similar to that of the 53 wt.% $CaCl_2$ solution, but this solution has a liquidus temperature of approximately 35 °C according to the phase diagram presented in Figure 3.

Experimental results

Deposit structure

A number of experiments have been carried out using a range of operational conditions,

examining the influence of solution composition, aqueous solution flow rate and bath temperature on freeze lining formation (see Table 2). A typical example of freeze lining growth in the current study is shown in Figure 4 (Experiment 1, Table 2). This experiment was carried out using a solution containing 53 wt.% $CaCl_2$, a bath temperature of 40 °C and a solution flow rate of 111 ml/min.

Table 2: List of experimental settings, times at which the white area was first observed, interface temperatures at the end of the experiments and solid phases present at the deposit/liquid interfaces. Experiments marked by '*' indicate experiments where the gap between the cooling plate and the tank was closed off using Norprene tubing.

Exp.	**wt.% $CaCl_2$ in solution**	**Solution flow rate (ml/min)**	**T_{bath} (°C)**	**Time at which white area was first observed**	**$T_{interface,end}$ (°C)**	**Phases at interface**
1	53	111	40	840	35.3	α
2	53	328	40	180	37.0	α
3*	53	328	40	10560	29.8	β
4	53	854	40	1920	36.9	α
5*	53	328	50	7440	29.5	β
6*	53	854	50	3240	/	α
7*	52	111	40	8880	29.4	β
8*	52	111	40	5520	34.7	α
9	52	111	40	2100	35.9	α
10	52	854	40	1320	35.5	α

At time zero, there is no deposit on the cooled copper plate. The first layer of freeze lining formed (β + L) was grey in appearance and grew evenly over the height of the cooled plate (see 0.27 h). After 0.53 h, a white area has appeared in the deposit, growing from a position at the rear of the cooled copper plate and increasing in size, as can be seen from the images obtained at 0.53, 0.80, 1.45 and 2.5 h. As the time progressed, the extent of this white region increased until it occupied the whole length of the deposit

from top to bottom, and also reached the deposit/liquid interface. At those locations where the white area reached the deposit/liquid interface, facetted grey crystals (α) were formed during subsequent growth of the deposit (0.80 h, 1.45 h). The thickness of the deposit continued to grow until the experiment was terminated after 41.0 h. No steady state was achieved. During growth of the freeze lining, the interface is non-planar due to the columnar growth of the α crystals, with each crystal forming a 'bump' on the interface, as can be see at 2.5h (Figure 4). As can be seen in Figure 4 (41 h), the lower section of freeze lining near the bottom of the tank formed a thicker deposit than on the upper part of the copper plate. The deposit/liquid interface temperature at the end of the experiment (41 h) was found to be 35.3°C. No detached crystals were observed in the liquid bath at any time during the experiment.

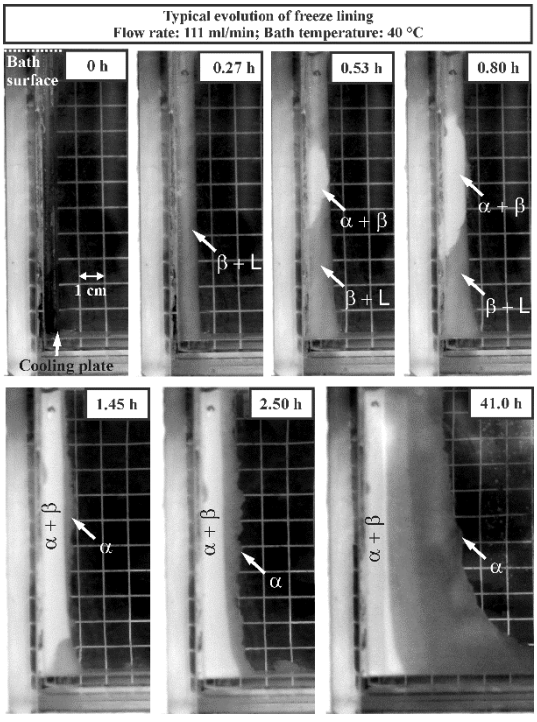

Figure 4: Freeze lining growth in a 53 wt.% CaCl2/water solution. Experiment was carried out using a bath temperature of 40 °C and a flow rate of 111ml/min.

Similar results were obtained for a 53 wt.% $CaCl_2$ solution, a bath temperature of 40 °C and fluid flow rates of 328 (experiment 2) and 850 (experiment 4) ml/min, and for a 52 wt.% $CaCl_2$ solution with a bath temperature of 40 °C and fluid flow rates of 111

(experiments 8*, 9) and 850 (experiment 10) ml/min; the interface temperatures in all of these cases were in the range of 34.7 to 37.0 °C.

The time and position at which the white area was first observed in the deposit on the copper plate was different for each experiment; it was unclear what causes or facilitates the formation of this layer, however, it was found that isolating the back of the copper plate from the bulk solution decreased the rate at which the white phase spread to the freeze lining that was in contact with the bulk solution. In experiments 3*, 5*, 6*, 7* and 8*, the apparatus was modified by inclusion of a barrier in the form of a Norprene rubber strip between the copper plate and the bath sidewall to limit the spread of the white area. In three of these experiments, thermal steady state was achieved in relatively short times (2 – 10 h, see Figure 5) and, in stark contrast to the other experiments, the temperature of the deposit/liquid interface of experiments 3*, 5* and 7* was found to be between 29.4 and 29.8 °C. Inspection of the phase diagram shown in Figure 3 shows that this corresponds to the upper limit of stability of the β $CaCl_2.6H_2O$ phase.

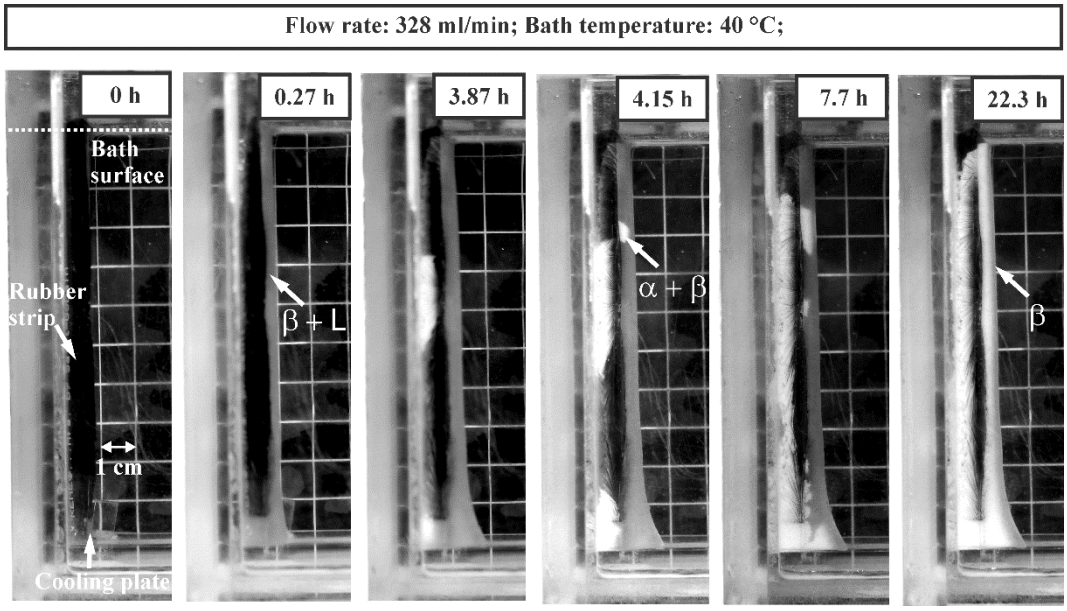

Figure 5: Freeze lining growth in a 53 wt.% CaCl2/water solution. Experiment 3* was carried out using a bath temperature of 40 °C and a flow rate of 328 ml/min. No layer of α was formed at the deposit/liquid interface. Steady state interface temperature was found to be 29.8 °C.

Subsequently, samples of the deposit formed in experiment 9, which formed a structure similar to that seen on Figure 4 (41 h), were taken for thermo-gravimetric analysis (TGA) (Crivits, 2016). It was found that the sample from the white layer had a bulk composition of 51.2 wt.% $CaCl_2$, which approximately corresponds to the bulk bath composition of 52 wt.% $CaCl_2$ in this experiment. According to the phase diagram shown in Figure 3, this bulk composition below the solidus would result in a mixture of the β phase, $CaCl_2.6H_2O$, and α phase, $CaCl_2.4H_2O$, assuming chemical equilibrium is achieved. In the same experiment, the composition of the crystals in the grey layer formed after the white layer had reached the deposit/liquid interface was determined to be 59.0 wt.% $CaCl_2$, which closely approximates the composition of the primary $CaCl_2.4H_2O$ phase, α, (60.6 wt.% $CaCl_2$). Cryo-SEM was also performed on these samples, but yielded no accurate quantitative results (Crivits, 2016).

In experiments (Exp 3*, 5*, 7*), in which the white layer never reached the deposit/liquid interface, the layer consisting solely of α CaCl2.4H2O was never formed. Due to interaction with the bulk bath, interconnectivity with the white area and hydration + melting when exposed to the atmosphere, no samples could be taken of the interface in these experiments. Based on the phase equilibria in the system (Figure 3) and the clear differences in the morphology of the layers (Figure 6), this layer is hypothesized to consist solely of β CaCl2.6H2O crystals.

Figure 6 shows a section of the deposit in which individual primary phase α, $CaCl_2.4H_2O$, crystals have nucleated and started to grow along the deposit/liquid interface. It can be seen that the α phase forms relatively large (0.3 cm diameter) facetted crystals and the interface is irregular in shape. In contrast, the first-formed β

interface exhibits a macroscopically smooth and even structure, producing a deposit layer of uniform thickness.

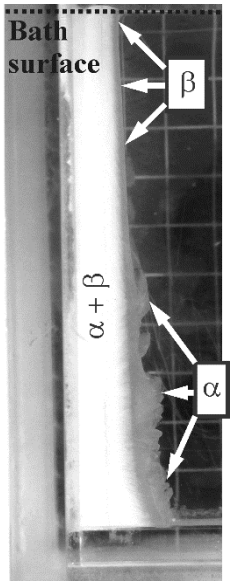

Figure 6: Deposit interface showing the formation and growth of primary phase α crystals across the original interface consisting of the β phase. Experiment was carried out in a 52 wt.% CaCl2 in water solution, bath temperature of 40 °C and solution flow rate of 111 ml/min.

Deposit thickness

The thicknesses of the deposits as a function of time are shown in Figure 7 and Figure 8. The thicknesses of the deposits were measured at the mid-height of the cooling plate at the same level as the dividing plate. A continuous line was used to represent the thickness over time, comprising of a (combination of) rational function(s) of the form $(a.t^2+b.t+c)/(t^2+d.t+e)$, where t represents the time, fitted to the data points using the least square method utilizing Matlab2013. This function was chosen for its asymptotical behaviour, representing the steady state behaviour of the freeze lining, and its close fit to the measured data, but has no further physical meaning.

It can be seen that in all cases, the rate of growth of the deposits decreases as the thickness increases. From the results obtained in experiments 1, 2, 4, 8*, 9 and 10

(Figure 7), it can be seen that there is no significant effect of solution fluid flow rate on deposit growth rate. Inspection of the deposit structure of experiments 4 and 8* shows that in these cases, the nucleation of the primary α phase was delayed relative to the other experiments. The dotted lines in these experiments represent estimated sections, based on the growth of the deposit in experiments with similar settings, where the primary phase was present at the interface. Whilst there are differences in the initial growth rates of the deposits, the steady state deposit thickness, approached at longer times for the solutions containing 52 wt.% $CaCl_2$ are, for these conditions, within the uncertainty of the experiments, independent of the fluid flow rate (Exp. 8*, 9, 10).

The steady state deposit thicknesses, in contrast, appear to be highly sensitive to solution concentration. In experiments 1, 2 and 4, the limiting values of deposit thickness for the solution containing 53 wt.% $CaCl_2$ appear to be approximately twice that of the solution containing 52 wt.% $CaCl_2$.

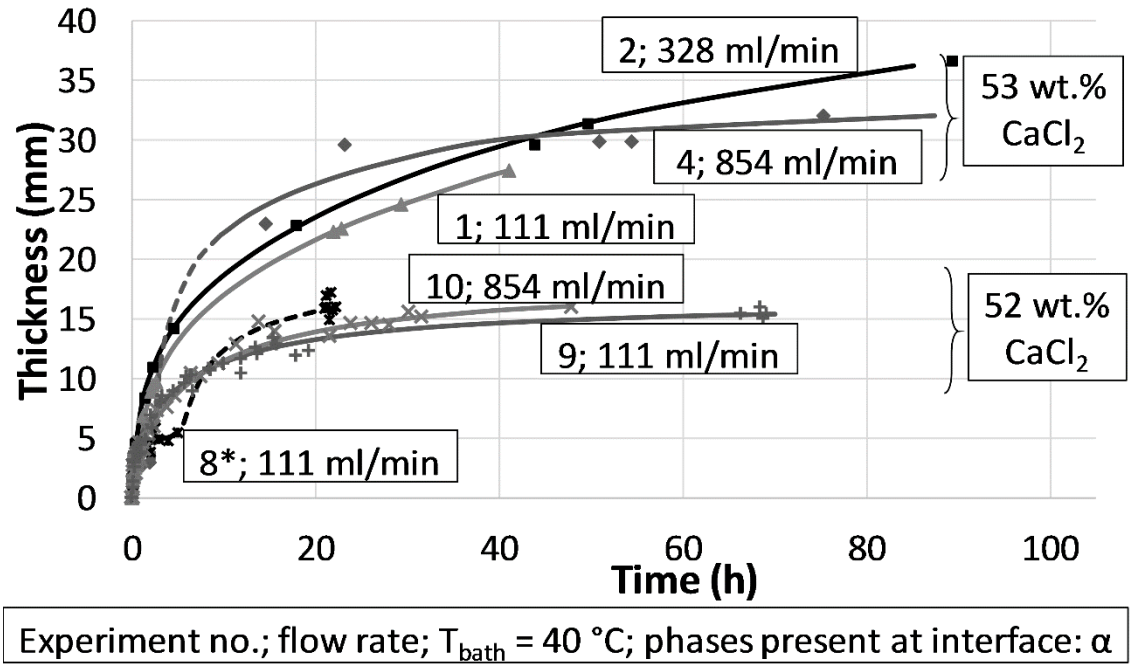

Figure 7: Deposit thickness as function of time for experiments 1, 2, 4, 8*, 9 and 10.

The thicknesses of the deposits as a function of time for experiments 3*, 5*, 6* and 7*

are shown in Figure 8. It can be seen that for experiments 3* and 7*, the steady state deposit thicknesses for the 52 and 53 wt.% $CaCl_2$ solutions respectively, having the β phase at the deposit/liquid interface, are significantly less than for conditions where the primary α phase layer is formed, for comparable solution flow and bath temperature conditions (experiments 2, 9).

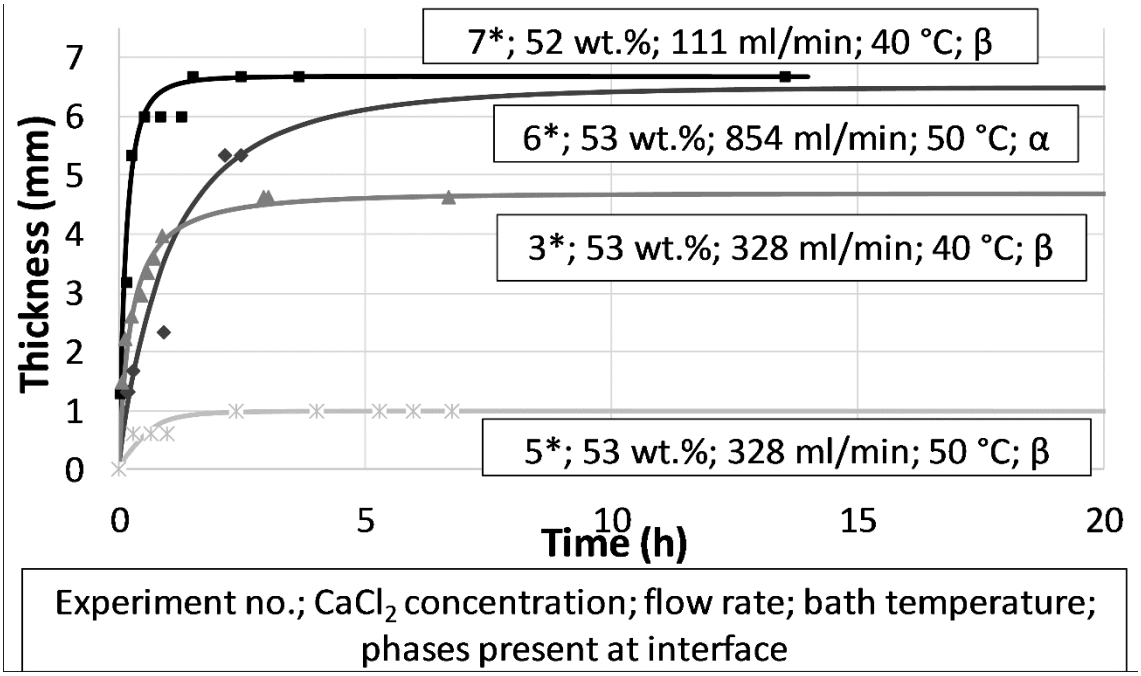

Figure 8: Deposit thickness as function of time for experiments 3*, 5*, 6* and 7*.

The effect of bath temperature can be seen from comparison of experiments 3* and 5* at 53 wt.% $CaCl_2$, having the β phase at the deposit/liquid interface, the deposit thickness for the higher bath temperature of 50 °C is significantly lower, than that for the bath at 40 °C.

The bath composition was not independently controlled at fixed composition. The total quantity of $CaCl_2$ in the system is fixed. As the deposit thickness increases, the $CaCl_2$ concentration in the aqueous solution changes. By undertaking a mass balance on the $CaCl_2$, the change in concentration can be calculated. Based on the total volume of solution (2.5 l) and the volume of the deposit when the deposit is 3.5 mm thick, the

solution contains between 52.5 and 53.2 wt.% $CaCl_2$ for a starting composition of 53 wt.% $CaCl_2$, depending on the relative proportion of α and β in the deposit. This represents the worst case scenario where the thickest observed freeze lining consists of 100% α or β. As such, the actual changes in composition during the experiments will be lower and are not expected to significantly influence the freeze lining behaviour.

The level of the solution was found to stay constant through experiments, suggesting negligible evaporation of water took place during the course of each experiment.

Discussion

Comparison with previous study

The current study differs in several ways from the study by (Guevara & Irons, 2011, Guevara & Irons, 2011) in the same system. As to the experimental apparatus, in the present study the geometry of the acrylic tank is different , and a peristaltic pump was used to induce forced convection as opposed to the natural convection used by (Guevara & Irons, 2011). Also, in the present study the use of a separate tank containing the heating element significantly increased the time which the solution spent at temperatures above the liquidus.

These differences in experimental set-up resulted in some new observations: (i) the formation of a white, 2-phase area, within the deposit; (ii) the formation of an α, $CaCl_2.4H_2O$, layer at the interface in some experiments as opposed to a β, $CaCl_2.6H_2O$, layer; (iii) the lack of any detached crystals in the bulk liquid, even at temperatures below the liquidus.

The lack of detached crystals in the liquid close to the interface, at temperatures below the liquidus, can not be explained by the equilibrium solidification model proposed by

(Guevara & Irons, 2011).

Influence of phases present at the deposit/liquid interface

The results of the present study (see Table 2, Figure 7, Figure 8) indicate differences in the steady state interface temperature and deposit thickness depending on the phase that is in direct contact with the liquid bath. To demonstrate this, the bath temperature of the 7* experiment was adjusted after reaching steady state at 13 h. At this point in time, a β layer was present at the interface (Table 2). The deposit was then partially dissolved by increasing the bath temperature to 50 °C to reveal the underlying α + β layer before returning again to the original bath temperature of 40 °C. The measured thickness of the freeze lining over time and the measured interface temperature at the top, middle and bottom of the freeze lining are shown on Figure 9. The exact position of the top, middle and bottom measurements have been indicated on Figure 10. The experiment was undertaken using the Norprene rubber seal to slow down the formation of the α + β layer (Figure 5).

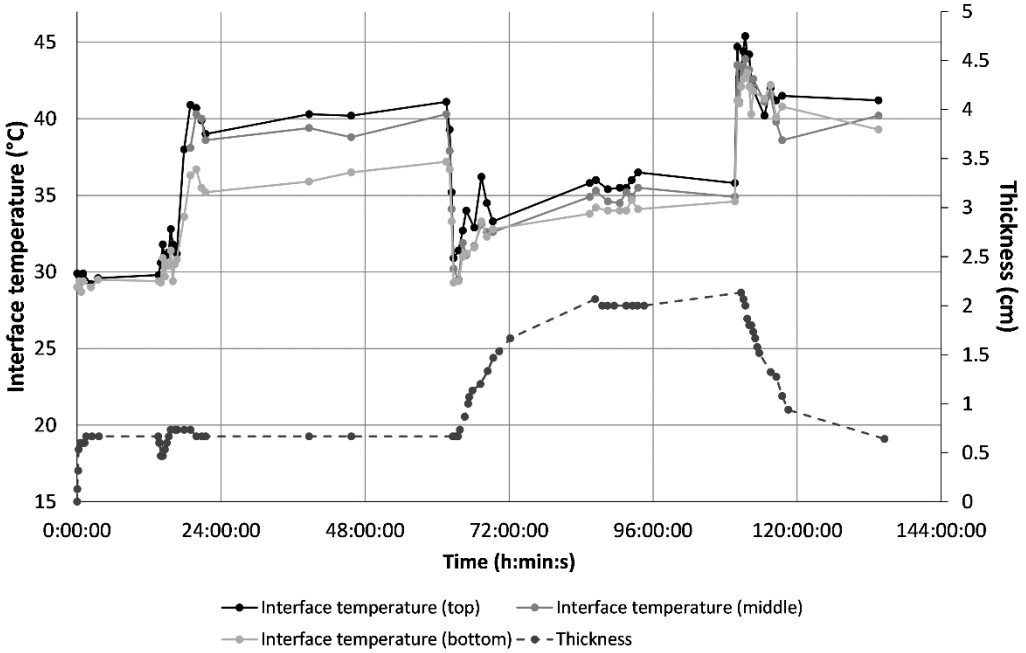

Figure 9: Measured interface temperatures at the top, middle and bottom of the freeze lining and the measured thickness of the freeze lining. The first 13 hours correspond to experiment 7*. Experiment was carried out in a 53 wt.% CaCl2/H2O solution at a flow rate of 111 ml/min. Bath temperature was changed as indicated on the upper side of the graph.

During the initial stage of this experiment, the bath temperature was set at 40 °C. The freeze lining grew rapidly until it reached a thickness of approximately 7 mm (experiment 7*). No measurements of the interface temperature were performed until the freeze lining had reached a thickness of 5 mm (0.33 h). After this initial growth, interface temperatures at the top and at the bottom of the freeze lining were found to be 29.6 and 29.2 °C respectively. Interface temperatures at this stage remained constant with time.

After 13 h, the temperature of the bath was increased to 50 °C. After an initial decrease in the thickness of the freeze lining, the freeze lining thickness increases to approximately 7 mm (see Figure 9, Figure 10). Interface temperatures during this growth phase increase over time.

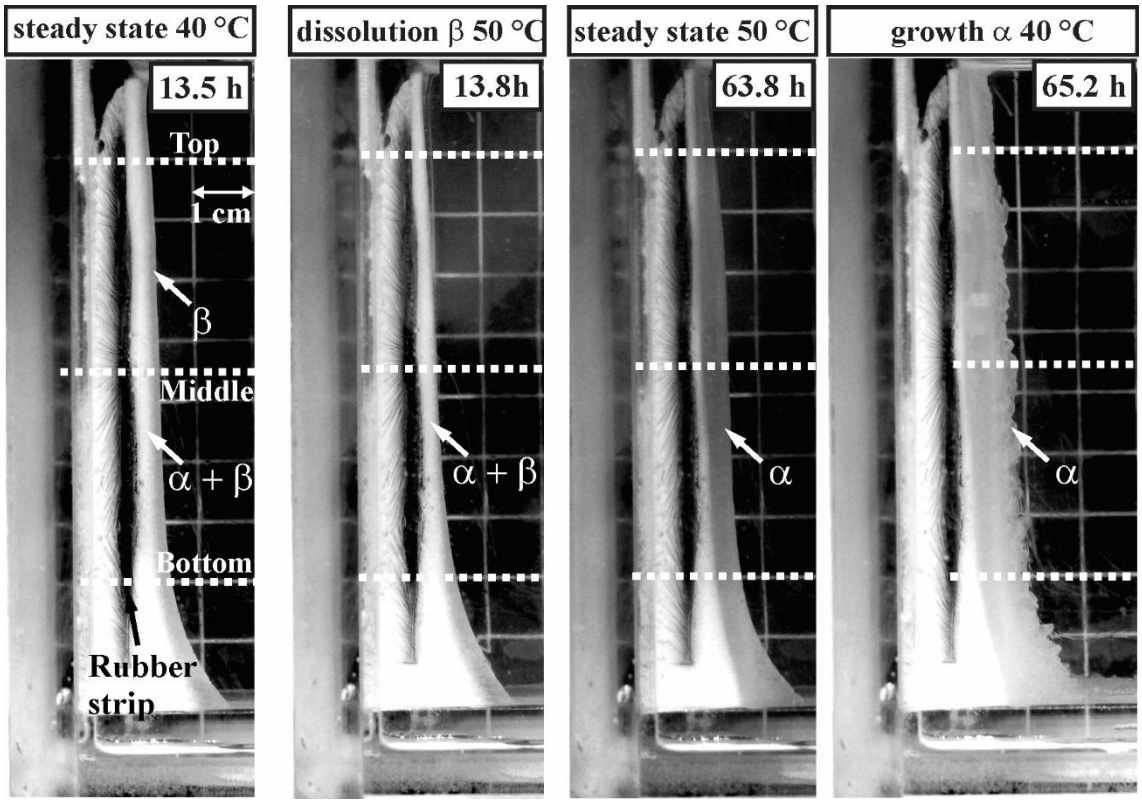

Figure 10: Evolution of freeze lining after increase and subsequent decrease in bath temperature. Experiment was carried out in a 53 wt.% $CaCl_2/H_2O$ solution at a flow rate of 111 ml/min. Bath temperature was changed as indicated on the upper side of the graph.

The subsequent decrease in temperature back to 40 °C after 60 h resulted in an increase in deposit thickness up to approximately 21 mm (see Figure 9, Figure 10). In the final step, the bath temperature was increased in temperature again to 50 °C after 108 h. The freeze lining partially dissolved back into the bath, decreasing the thickness to approximately 6 mm, which was within uncertainty of the thickness observed between 15 and 63 h. The measured interface temperatures after 108 h initially increased to values significantly above the steady state interface temperatures measured earlier at a bath temperature of 50 °C. Subsequently, interface temperatures dropped and reached values comparable to that observed between 20 and 63 h.

The results can be explained as follows: The β sealing layer formed initially at the deposit/liquid interface between 2 and 12 h was metastable. By changing the bath

temperature from 40 °C to 50 °C, the metastable sealing layer was dissolved and replaced by a primary α phase sealing layer. When decreasing the bath temperature to 40 °C again, the primary phase sealing layer grew further, creating a much thicker freeze lining comparable to that observed in experiments 1, 2 and 4 in which the α phase was clearly identified.

The experiment indicates that once the initial metastable β layer has been dissolved, it does not reform when returning to the original conditions due to the formation of an α sealing layer.

Metastability of freeze linings

In a previous study (Guevara & Irons, 2011), detached crystals were observed in the liquid at subliquidus temperatures. Based on this observation, a numerical model was proposed assuming equilibrium solidification (Guevara & Irons, 2011). In the current study, no detached crystals were observed in the liquid adjacent to the freeze lining deposit, even when the interface temperature was well below the liquidus (Exp. 4*, 5*, 8*). As a result, the assumption of equilibrium solidification is not valid for the investigated conditions.

The results can be explained by considering a dynamic steady state, as proposed by (Fallah-Mehrjardi, Hayes & Jak, 2013). If, in the investigated system, the growth kinetics of the primary and secondary phases are such that the secondary β, $CaCl_2.6H_2O$, phase precipitates first (Figure 12b, c), and the subsequent nucleation/growth of the primary $CaCl_2.4H_2O$ phase (α) is slow compared to the mass transfer of material towards the deposit (i.e. the system follows the crystallization path on the metastable phase diagram in Figure 11), the secondary β phase forms a sealing crystal layer before the primary α phase reaches the interface (Figure 12c). As no

primary phase is present at the interface, the freeze lining stops growing when the interface temperature equals the temperature at which the secondary $CaCl_2.6H_2O$ phase becomes stable, that is, the liquidus temperature in the metastable system excluding the formation of $CaCl_2.4H_2O$ (Figure 11). It can be observed from Figure 11 that this temperature is approximately 29 °C, which is within the experimental uncertainty of the solidus temperature of 29.9 °C on the stable phase diagram (Figure 3).

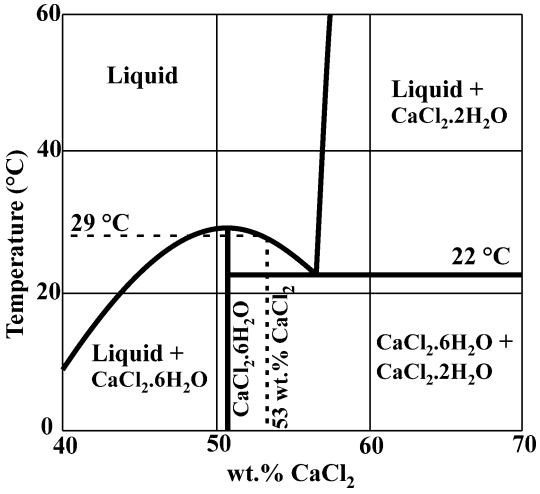

Figure 11: Estimated metastable phase diagram at the conditions of interest, excluding the formation of $CaCl_2.4H_2O$.

Moreover, any primary $CaCl_2.4H_2O$ (α) crystals that do eventually nucleate in the liquid close to the deposit interface at subliquidus temperatures keep circulating in the bath, eventually dissolving back into the bulk bath liquid, at temperatures above the liquidus temperature.

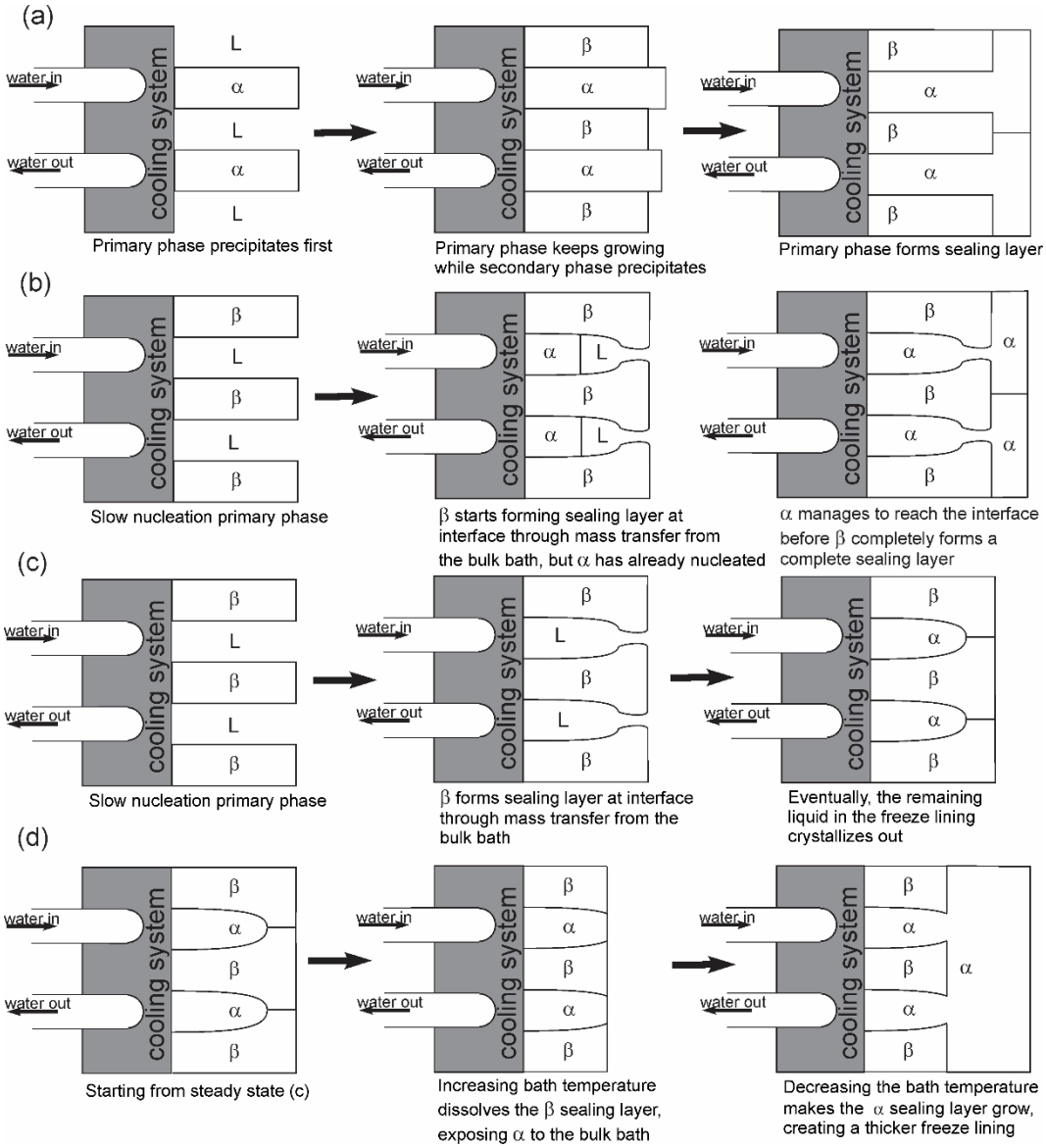

Figure 12: Hypothesized microstructural changes during freeze lining formation. (a) Expected growth of the freeze lining, with the primary phase α precipitating first; (b) The formation of the primary α phase is slow, resulting in the partial closure of the β layer at the interface; (c) Dynamic steady state model where the formation of the primary α phase is inhibited. As a result, the secondary β phase forms a sealing layer; (d) Evolution of the freeze lining formed in (c) after an increase and subsequent decrease in bath temperature.

The detached crystals observed in earlier experiments (Guevara & Irons, 2011) can then be explained by considering the relatively short time detached crystals spent in the area with temperature above the liquidus. As such, these crystals, once nucleated, never dissolved completely and kept circulating in the bath.

As has been shown in the previous section (Figure 9, Figure 10), increasing the bath temperature after formation of the β sealing layer dissolves this sealing layer, exposing the primary α crystals to the bulk bath. Subsequently, the primary α phase grows and forms a sealing layer (Figure 12d). Upon decreasing the bath temperature to its original value, this primary α sealing layer grows further, increasing the thickness of the freeze lining beyond its original thickness, to the same steady state thickness as in Figure 12a and b.

Liquification of intermediate layers

Inspection of Figure 13a shows that the local bulk composition in the freeze lining changes with increasing distance from the cooling system. It is interesting to consider what happens after increasing the bath temperature and/or agitation of the bath.

As mass transfer in the solid freeze lining is limited, the local bulk composition in the freeze lining will stay constant. As the agitation of the bath and/or the bath temperature increases, the thermal gradient inside the freeze lining will increase, evolving towards a new thermal steady state, according to the equation:

$$Q_{FL} = h_{bath} A_{bath,FL} \left(T_{bath} - T_{bath,FL}\right) = k_{FL} A_{bath,FL} \frac{dT}{dx} \qquad (4)$$

Assuming the temperature at the cold face stays constant, the local temperature in the freeze lining will thus increase.

If the increase in bath temperature/agitation is sufficiently high, part of the freeze lining containing the β phase can reach a local temperature higher than the local solidus temperature. As a result, this layer (partly) liquefies, as is demonstrated in Figure 13b, that is, the reaction β → α + L takes place.

This hypothesis was tested by increasing the bath temperature after conclusion of experiment 10 to 47 °C. It was found that a layer of the freeze lining liquefied, as is demonstrated in Figure 13c by inserting tweezers in the liquid gap.

The result of the liquification of this intermediate layer in the freeze lining is a reduction in the mechanical stability of the freeze lining. This is demonstrated in Figure 13c, where the impact of one of the 1mm diameter K-type thermocouples is enough to break off part of the freeze lining.

Assuming a constant coolant temperature, it can be shown that liquification occurs when the current temperature gradient is higher than the original temperature gradient in the freeze lining when a metastable β sealing layer was present, that is:

$$\frac{h_{bath,2}\left(T_{bath,2}-T_{bath,FL,2}\right)}{h_{bath,1}\left(T_{bath,1}-T_{bath,FL,1}\right)} > 1 \qquad (5)$$

Where $h_{bath,1}$ and $h_{bath,2}$, $T_{bath,1}$ and $T_{bath,2}$, $T_{bath,FL,1}$ and $T_{bath,FL,2}$ represent the initial and current convective heat transfer coefficient of the bath, temperature of the bath, and temperature at the bath-freeze lining interface.

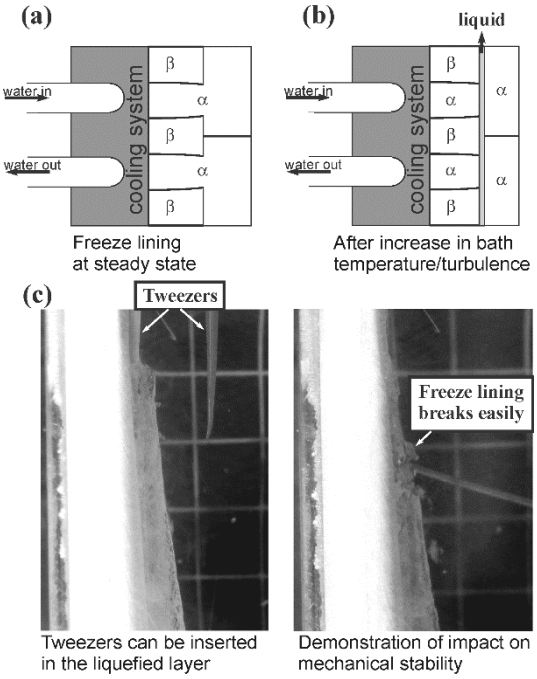

Figure 13: Liquification of intermediate freeze lining layers: (a) freeze lining at steady state, (b) freeze lining after an increase in bath temperature and/or turbulence (c) demonstration of the impact of liquification of the intermediate layer on the mechanical stability of the freeze lining.

Conclusions

The present study of freeze lining formation confirms previous observations that the deposit/liquid interface temperatures in these systems can be below those anticipated from chemical equilibrium considerations. This being the case, the formation of freeze linings can exhibit a range of behaviours from equilibrium to dynamic steady state. The departure from thermodynamic or chemical equilibrium means that steady state freeze lining behaviour is determined by not only heat transfer and thermal factors, but also by the relative rates of mass transfer and elementary reaction steps, such as nucleation, crystallisation rate, crystallisation pathway, phase transformations and phase equilibria in the reaction system.

In the present study, freeze lining behaviour in concentrated $CaCl_2$ containing aqueous solutions was studied through in-situ experimental observations. The influence of bath composition, bath temperature, fluid flow rate and thermal history have been investigated. The system behaviour was not noticeably influenced by differences in bulk fluid flow. It has been clearly shown, however, that the phases formed, the interface temperatures and the freeze lining thicknesses are highly sensitive to parameters that determine the chemical driving forces for change as reflected in the bath temperature, the bath composition and the thermal history of the deposit. These are significant findings since they are not predicted using conventional thermal treatment of freeze lining behaviour, and point to the need for further systematic examination of the influence of the various process parameters that affect the elementary reaction steps that may be active in these systems under dynamic steady state conditions.

Acknowledgements

The authors would like to thank the Australian Research Council ARC Discovery program and Umicore for the financial support for this research. The authors also thank UQ International Scholarship (UQI) program for providing a scholarship for T. Crivits. The authors acknowledge the facilities, and the scientific and technical assistance, of the Australian Microscopy & Microanalysis Research Facility at the Centre for Microscopy and Microanalysis, The University of Queensland.

References

Marx, F., Shapiro, M. & Henning, B. 'Application of high intensity refractory cooling systems in pyrometallurgical vessel design', in *12th Int. Ferroalloys Congr.*, (Helsinki, Finland: SAIMM, 2010).

Fallah-Mehrjardi, A., Jansson, J., Taskinen, P., Hayes, P. C. & Jak, E. 2014. Investigation of the Freeze-Lining Formed in an Industrial Copper Converting Calcium Ferrite Slag. *Metall. Mater. Trans. B*, 45B(864-74.

Fallah-Mehrjardi, A., Hayes, P. C. & Jak, E. 2014. Investigation of freeze-linings in aluminum production cells. *Metall. Mater. Trans. B*, 45(4):1232-47.

Blancher, S., B., Sayasenh, A. & Crespo, E. 'Follow-up and mineralogical characterization of freeze lining evolution: a record of furnace life', in *Metal 2015*, (Brno, Czech Republic: Tanger Ltd., 2015).

Fallah-Mehrjardi, A., Hayes, P. C. & Jak, E. 2013. Investigation of freeze linings in copper containing slag systems: Part II. Mechanism of the deposit stabilization. *Metall. Trans. B*, 44B(549-60.

Fallah-Mehrjardi, A., Hayes, P. C. & Jak, E. 2013. Investigation of Freeze linings in copper containing slag systems: Part I. Preliminary Experiments. *Metall. Trans. B*, 44B(534-48.

Fallah-Mehrjardi, A., Hayes, P. C. & Jak, E. 2013. Investigation of freeze lining in copper-containing slag systems: Part III. High-temperature experimental investigation of the effect of bath agitation. *Metall. Mater. B*, 44B(1337-51.

Fallah-Mehrjardi, A., Hayes, P. C. & Jak, E. 2014. Understanding slag freeze linings. *JOM*, 66(9):1654-63.

Kalliala, O., Kaskiala, M., Suortti, T. & Taskinen, P. 2015. Freeze lining formation on water cooled refractory wall. *Mineral Processing and Extractive Metallurgy*, 124(4):224-32.

Thonstad, J. & Rolseth, S. 'Equilibrium between bath and side ledge in aluminium cells. basic principles', in *Light Met.*, ed. By Adkins, E. M.: TMS, 1983), pp. 415-24.

Verscheure, K., Kyllo, A. K., Filzwieser, A., Blanpain, B. & Wollants, P. 'Furnace Cooling Technology in Pyrometallurgical Processes', in *Sohn International Symposium*, (San Diego, California: TMS, 2006), pp. 139-54.

Jansson, J., Taskinen, P. & Kaskiala, M. 2014. Freeze lining formation in continuous converting calcium ferrite slags. II. *Can. Met. Quart.*, 53(1):11-16.

Taylor, M. P. & Welch, B. J. 1987. Melt/freeze heat transfer measurements in cryolite-based electrolytes. *Metall. Trans. B*, 18B(3):391-98.
Pistorius, P. C. 2004. Equilibrium interactions between freeze lining and slag in ilmenite smelting. *J. S. Afr. I. Min. Metall.*, 104(417-22.
Zietsman, J. H. 2004. Interactions between freeze lining and slag bath in ilmenite smelting, PhD thesis, University of Pretoria.
Guevara, F. J. & Irons, G. A. 2011. Simulation of Slag Freeze Layer Formation: part II: Numerical Model. *Metall. Mater. Trans. B*, 42B(664-76.
Fallah-Mehrjardi, A. 2013. Investigation of freeze-lining formation in metallurgical systems, PhD Thesis, University of Queensland.
Fallah-Mehrjardi, A., Hayes, P. C. & Jak, E. 2014. Further Experimental Investigation of Freeze-Lining/Bath Interface at Steady-State Conditions. *Met. Trans. B*, 45(6):2040-49.
Hayes, P.C. 2013. Reaction Kinetics. In: Editor EE, editor(s). Treatise on Process Metallurgy – volume 1 – Process Fundamentals. Place: Publisher; p. pages.
Welty, J. R., Wicks, C. E., Wilson, R. E. & Rorrer, G. L. 2007. *Fundamentals of Momentum, Heat, and Mass Transfer.* USA: Wiley.
Gardon, R. 1961. A Review of Radiant Heat Transfer in Glass. *J. Am. Ceram. Soc.*, 44(7):305-12.
Campforts, M., Blanpain, B. & Wollants, P. 2009. The Importance of Slag Engineering in Freeze Lining Applications. *Metall. Mater. Trans. B*, 40(5):643-55.
Solheim, A. & Thonstad, J. 'Heat transfer coefficients between bath and side ledge in aluminum cells. model experiments', in *Light Met.*, ed. By Adkins, E. M.: TMS, 1983), pp. 425-35.
Solheim, A. & Thonstad, J. 1984. Model experiments of heat transfer coefficients between bath and side ledge in aluminum cells. *Journal of Metals*, 36(3):51-55.
Bruggeman, J. N. & Danka, D. J. 'Two-dimensional thermal modeling of the hall-héroult cell', in *Light Met.*, ed. By Bickert, M.: TMS, 1990), pp. 203-09.
Chen, J. J. J., Wei, C. C., Thomson, S., Welch, B. J. & Taylor, M. P. 'A study of cell ledge heat transfer using an analogue ice-water model.', in *Light Met.*, ed. By Mannweiler, U.: TMS, 1994), pp. 285-93.
Valles, A. & Lenis, V. 'Prediction of ledge profile in hall-héroult cells.', in *Light Met.*, ed. By Evans, J.: TMS, 1995), pp. 309-13.
Wei, C. C., Chen, J. J. J., Welch, B. J. & Voller, V. R. 'Modelling of dynamic ledge heat transfer', in *Light Met.*, ed. By Huglen, R.: TMS, 1997), pp. 309-16.
Solnordal, C. B., Jorgensen, F. R. A. & Taylor, R. N. 1998. Modeling the heat flow to an operating sirosmelt lance. *Metall. Mater. Trans. B*, 29(2):485-92.
Robertson, D. G. C. & Kang, S. 'Model studies of heat transfer and flow in slag-cleaning furnaces', in *TMS Annual Meeting, Fluid Flow Phenomena in Minerals Processing*, ed. By El-Kaddah, N., Robertson, D. G. C., Johansen, S. T. and Voller, V. R., (San Diego, California: TMS, 1999), pp. 157-68.
Thonstad, J., Fellner, P., Haarberg, G. M., Hives, J., Kvande, H. & Sterten, A. 2001. *Aluminium Electrolysis: Fundamentals of the Hall-Héroult Process.* 3rd edition ed. Düsseldorf: Aluminium-Verlag GmbH.
Solheim, A. 'Coupled heat and mass transfer during melting or freezing of sideledge in aluminium cells.', in *12th Aluminium Symposium, Bratislava, Slovakia*, 2003).
Solheim, A. 'Some aspects of heat transfer between bath and sideledge in aluminium reduction cells', in *Light Metals*, ed. By Lindsay, S. J.: TMS, 2011), pp. 381-86.
Guevara, F. J. & Irons, G. A. 2011. Simulation of Flag Freeze Layer Formation: Part 1. Experimental Study. *Metall. Mater. Trans. B*, 42B(652-63.

Thonstad, J. & Rolseth, S. 'Equilibrium between bath and side ledge in aluminiium cells. basic principles', in *Light Met.*, ed. By Adkins, E. M.: The Metallurgical Society of AIME, 1983), pp. 415-24.
Fallah-Mehrjardi, A., Hayes, P. C., Vervynckt, S. & Jak, E. 2014. Investigation of freeze-linings in a nonferrous industrial slag. *Metall. Mater. Trans. B*, 45(3):850-63.
Rasbane, W. S. 'ImageJ', (Bethesda, Maryland, USA: U.S. National Institutes of Health, 1997-2015).
Conde-Petit, M. R. 2014. *Aqeous solutions of lithium and calcium chlorides: property formulations for use in air conditioning equipment design.* Zurich, Switzerland: M. Conde Engineering.
DOWChemical 2002. *Calcium chloride handbook: a guide to properties, forms, storage and handling.* Midland, MI.
Crivits, T. 2016. Fundamental studies on the chemical aspects of freeze linings, PhD thesis, University of Queensland.